



This open access document is posted as a preprint in the Beilstein Archives at <https://doi.org/10.3762/bxiv.2020.133.v1> and is considered to be an early communication for feedback before peer review. Before citing this document, please check if a final, peer-reviewed version has been published.

This document is not formatted, has not undergone copyediting or typesetting, and may contain errors, unsubstantiated scientific claims or preliminary data.

Preprint Title Synthesis and physicochemical evaluation of fluorinated lipopeptide precursors of ligands for microbubble targeting

Authors Masayori HAGIMORI, Estefania E. MENDOZA-ORTEGA and Marie Pierre KRAFFT

Publication Date 26 Nov 2020

Article Type Full Research Paper

Supporting Information File 1 Hagimori.SI.BOJC.26.11.20.docx; 570.7 KB

ORCID® iDs Marie Pierre KRAFFT - <https://orcid.org/0000-0002-3379-2783>

License and Terms: This document is copyright 2020 the Author(s); licensee Beilstein-Institut.

This is an open access publication under the terms of the Creative Commons Attribution License (<https://creativecommons.org/licenses/by/4.0>). Please note that the reuse, redistribution and reproduction in particular requires that the author(s) and source are credited.

The license is subject to the Beilstein Archives terms and conditions: <https://www.beilstein-archives.org/xiv/terms>.

The definitive version of this work can be found at <https://doi.org/10.3762/bxiv.2020.133.v1>

1 Synthesis and physicochemical evaluation of fluorinated
2 lipopeptide precursors of ligands for microbubble targeting

3 Masayori Hagimori,^{1,2,3 †*} Estefanía E. Mendoza-Ortega,¹ Marie Pierre Krafft^{1*}

4 ¹Institut Charles Sadron (CNRS), University of Strasbourg, 23 rue du Loess, 67034
5 Strasbourg CEDEX 2, France

6 ²Faculty of Pharmaceutical Sciences, Mukogawa Women's University, 11-68 Koshien
7 Kyubancho, Nishinomiya 663-8179, Japan

8 ³Graduate School of Biomedical Sciences, Nagasaki University, 1-7-1 Sakamoto,
9 Nagasaki 852-8501, Japan

10

11 Corresponding authors:

12 Dr. M. Hagimori: hagimori@mukogawa-u.ac.jp

13 Dr. M.P. Krafft: krafft@unistra.fr

14 *†This work was achieved during a stay of M. H. at the Institut Charles Sadron*
15 *(Strasbourg).*

16 Keywords: perfluoroalkylated lipopeptide; solid-phase peptide synthesis; monolayer;
17 adsorption at fluid interfaces; microbubble targeting; molecular imaging, drug delivery

18

1 Abstract

2 Ligand-targeted microbubbles are focusing interest for molecular imaging and delivery
3 of chemotherapeutics. Novel lipid-peptide conjugates (lipopeptides) that feature
4 alternating serine-glycine (SG)_n segments rather than the classical poly(oxyethylene)
5 chains as linkers between the polar head of the lipid and a targeting ligand were recently
6 proposed for liposome-mediated, selective delivery of anti-cancer drugs. Here, we report
7 the synthesis of perfluoroalkylated lipopeptides (*F*-lipopeptides) bearing two
8 hydrophobic chains (C_nF_{2n+1}, *n* = 6, 7, 8, **1-3**) grafted through a lysine moiety on a
9 hydrophilic chain composed of a lysine-serine-serine (KSS) sequence followed by 5 SG
10 sequences. These *F*-lipopeptides are precursors of targeting lipopeptide conjugates. A
11 hydrocarbon counterpart with a C₁₀H₂₁ chain (**4**) was synthesized for comparison. The
12 capacity for the *F*-lipopeptides to spontaneously adsorb at the air/water interface and to
13 form monolayers in combination with dipalmitoylphosphatidylcholine (DPPC) was
14 investigated. The *F*-lipopeptides **1-3** demonstrated a markedly enhanced tendency to form
15 monolayers at the air/water interface, with equilibrium surface pressures reaching ~7-10
16 mN m⁻¹ as compared to less than 1 mN m⁻¹ only for their hydrocarbon analog **4**. The *F*-
17 lipopeptides penetrate in the DPPC monolayers in both liquid expanded (LE) and liquid
18 condensed (LC) phases without interfacial film destabilization. By contrast, the
19 hydrocarbon analog provokes delipidation of the interfacial film. The commercial
20 microbubble-based products used for contrast ultrasound imaging are all stabilized by a
21 fluorocarbon gas. The ability of the *F*-lipopeptides to integrate fluorocarbon-stabilized
22 phospholipid-shelled microbubbles was studied. Incorporation of *F*-lipopeptides **1-3** in
23 microbubbles with a shell of DPPC and dipalmitoylphosphatidylethanolamine-PEG2000
24 decreased their mean diameter and increased their stability, the best results being obtained
25 for the C₈F₁₇-bearing lipopeptide **3**. By contrast, incorporation of the hydrocarbon
26 lipopeptide led to microbubbles with a larger mean diameter, and significantly lower
27 stability.

28

1 Introduction

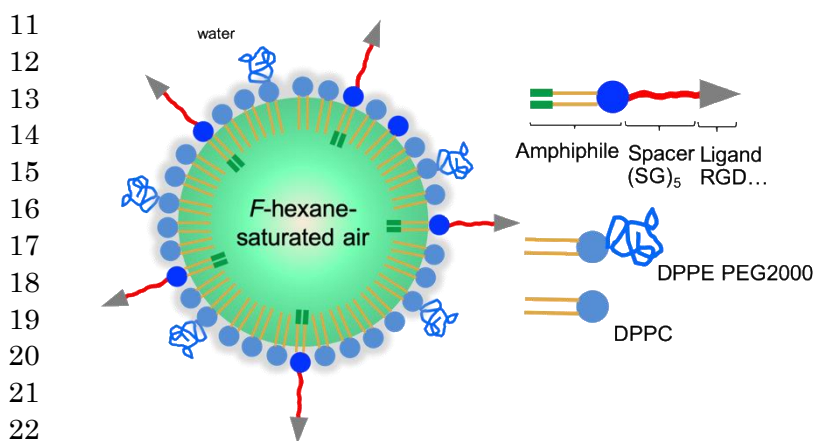
2 Various nano- and microsystems, including micelles, liposomes and microbubbles,
3 have been developed as imaging agents and to selectively deliver chemotherapeutics to
4 tumor cells [1-6]. Increased specificity for tumor cells can be gained through ligand-
5 mediated active targeting, which involves the use of targeting ligands, such as monoclonal
6 antibodies, antibody fragments, proteins, peptides, and other small molecules, including
7 vitamins and carbohydrates [7, 8]. The targeting ligands are coupled to the surface of the
8 carrier to selectively target tumor cells that overexpress a particular cell surface receptor
9 [7, 9-12]. To this aim, ligand-lipid conjugates have been developed in research and
10 preclinical development for liposome targeting for decades. In particular, peptide ligands
11 offer significant advantages, including efficient synthesis routes, versatility and safety
12 [13-15]. Various effective receptor-binding peptides have been identified by phage
13 display technology [16]. The peptides can be readily prepared through solid-phase peptide
14 synthesis (SPPS), a highly reproducible method with minimal side reactions. Many
15 peptide-lipid conjugates (lipopeptides) have been used as amphiphilic components of
16 drug delivery systems with anti-cancer properties, such as the tripeptide Arg-Gly-Asp
17 (RGD) that binds to integrin $\alpha_v\beta_3$, which is expressed on endothelial cells of various
18 malignant tumors [13, 17-20]. Other lipopeptides display cell penetrating properties, such
19 as the transactivator of transcription (TAT) peptide. Moreover, peptides being smaller than
20 antibodies generally induce lower immunogenicity [13-15]. Micro- and nanocarriers are
21 often covered by poly(ethylene glycol) (PEG) stealth coatings that significantly enhance
22 blood circulation times by allowing them to evade immune detection. PEGs often plays a
23 key role in the design of the ligands as a spacer between the nanocarrier surface and the
24 lipid. PEGs have, however, some shortcomings, such as a broad molecular weight

1 distribution, large steric hindrance and the occurrence of side reactions due to reactive
2 groups introduced during PEG to lipids (or peptides) connecting reactions [21-23]. In
3 particular, the PEG layer grafted on the surface of certain nanocarriers restricts the
4 exposure of functional peptides [24, 25].

5 Novel ligand-grafted lipids have been proposed for the preparation of functional drug
6 carriers for clinical applications [23, 26, 27]. In order to alleviate the steric hindrance
7 effect of PEG chains, a novel spacer consisting of alternating serine-glycine sequences
8 (SG) $_n$ was introduced between the ligand and lipid within the molecular structure [28].
9 These lipopeptides have a discrete molecular weight and are produced by Fmoc
10 (fluorenylmethoxycarbonyl protecting group) SPPS, a procedure in which the peptide
11 chain is assembled stepwise while attached to an insoluble resin support, which allows
12 easy removal of the by-products at each step by washing. Human epidermal growth factor
13 receptor-2 (HER2)-targeting KCCYSL peptide-(SG) $_n$ -lipids in which the (SG) $_n$ ($n = 3, 5,$
14 7) sequence was used as a spacer allowed reduction of steric hindrance when compared
15 to the conventional PEG2000 spacer [26]. Liposomes containing these peptide ligands
16 dramatically increased cellular association in HER2-positive cells. Other lipids grafted to
17 the RGD peptide and SG spacer were integrated in PEGylated liposomes and were
18 efficiently associated with integrin $\alpha_v\beta_3$ -expressing Colon-26 cells [23].

19 One of our general objectives is to synthesize lipopeptides specifically designed for
20 incorporation in the phospholipid shell of medical microbubbles (MBs) (Scheme 1).
21 DPPC is widely used in the formulation of MBs, often in combination with a PEGylated
22 dipalmitoylphosphatidylethanolamine (DPPE-PEG2000) that further enhances MB
23 stability [29-31]. It is noteworthy that most of the phospholipid-stabilized MBs
24 investigated in research and preclinical development are stabilized by a fluorocarbon

1 (FC) gas [12, 29, 32]. FCs are known to contribute to MB stabilization through osmotic
 2 effect [29]. In addition, FCs were also found to act as co-surfactants to the phospholipid
 3 molecules of the MB shell and strongly reduce its interfacial tension.[33, 34] Recent
 4 studies have reported that the fluorine-fluorine interactions that develop between the FC
 5 and the MB shell component (*e.g.* fluorinated biomarkers [35] and fluorinated
 6 nanoparticles, including dendronized iron oxide nanoparticles [36] and nanodiamonds
 7 [37] efficiently reinforce the interfacial film cohesion, thus enhancing the stability of the
 8 MBs. Various types of perfluoroalkylated amphiphiles have been reported that were
 9 designed for biomedical applications and display highly effective nanoemulsion and MB
 10 stabilizing characteristics [38-40].



23 **Scheme 1.** Schematic representation of a perfluorohexane-stabilized microbubble with a
 24 fluorinated lipopeptide anchored in its phospholipid shell.

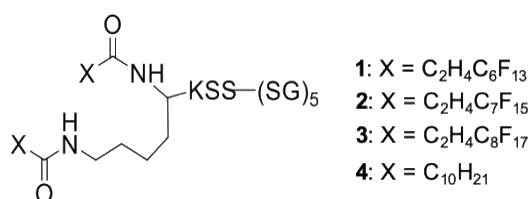
25 In this work, we report the synthesis of a series of *F*-lipopeptides that are precursors of
 26 targeting lipopeptide conjugates and are specifically designed to be incorporated in the
 27 shell of phospholipid microbubbles. In a first step, the (SG)₅KSS peptide chain is
 28 assembled stepwise using a Fmoc solid-phase peptide synthesis procedure. In a second
 29 step, the two perfluoroalkylated chains are grafted to the peptide chain through a lysine
 30 moiety. Next, the surface activity of the synthesized lipopeptides is investigated by

1 assessing their ability to self-assemble into spontaneously adsorbed monolayers at the
2 air/water interface and also to adsorb on a DPPC monolayer spread at the air/water
3 interface. Finally, the size and stability characteristics of perfluorohexane (*F*-hexane)-
4 stabilized microbubbles with DPPC/DPPE-PEG2000 shells and incorporating the new *F*-
5 lipopeptides were determined and compared to those of reference MBs of similar
6 phospholipid composition.

7 Results and Discussion

8 Synthesis and characterization of the lipid-peptide conjugates

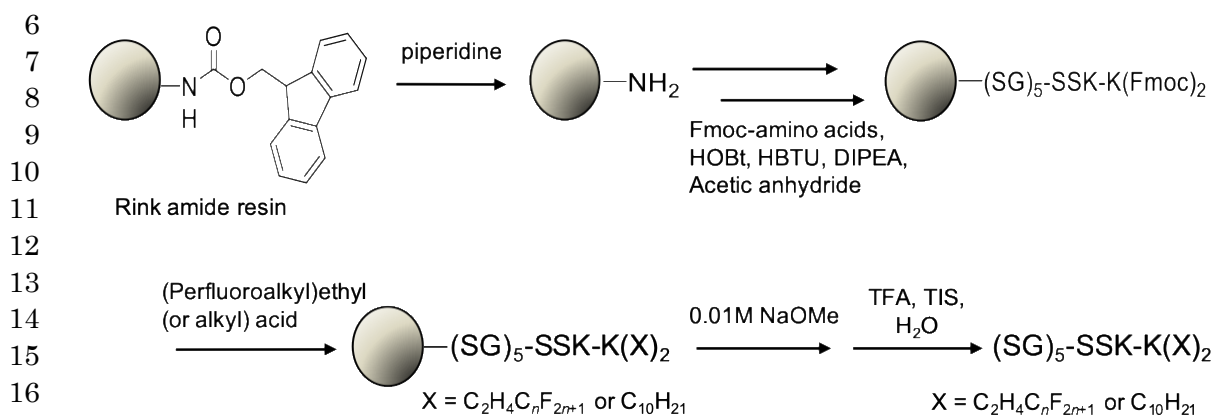
9 Since the degree of fluorination of the hydrophobic chains of the lipid conditions the
10 extent of fluorous interactions developed with the *FC* gas, we have selected various
11 perfluoroalkyl chain lengths (C_6F_{13} , C_7F_{15} , and C_8F_{17}). The length of the (SG) n sequence
12 was set to $n = 5$, which was found optimal in a previous report [26]. We synthesized three
13 perfluoroalkylated double-chain peptide-lipid conjugates, (SG) $_5$ -KSS-K($C_2H_4-C_nF_{2n+1}$) $_2$
14 with $n = 6$ (**1**), 7 (**2**) and 8 (**3**) (Scheme 2). The hydrocarbon analog fitted with two $C_{10}H_{21}$
15 chains (**4**) was also prepared.



23 **Scheme 2.** Structures of the perfluoroalkylated lipopeptides **1-3** and of their hydrocarbon
24 analog **4**.

25 The *F*-lipopeptide conjugates **1-3** and hydrocarbon analog **4** were obtained by a Fmoc
26 solid-phase peptide synthesis method, in which the peptide sequence was stepwisely
27 elongated, and eventually conjugated with the (perfluoroalkyl)ethyl acids (Scheme 3).

1 After cleavage from the resin, the Fmoc groups of the amino acids were removed, and the
 2 *F*-lipopeptides were purified using a dialysis membrane. According to mass spectrometry
 3 and HPLC-UV analysis, the products (**1-3**) had high purity (> 99%) (*Supporting*
 4 *Information* Figures S1-6). We also obtained the hydrocarbon analog **4** in high purity (>
 5 99%) (*Supporting Information* Figures S7,8).



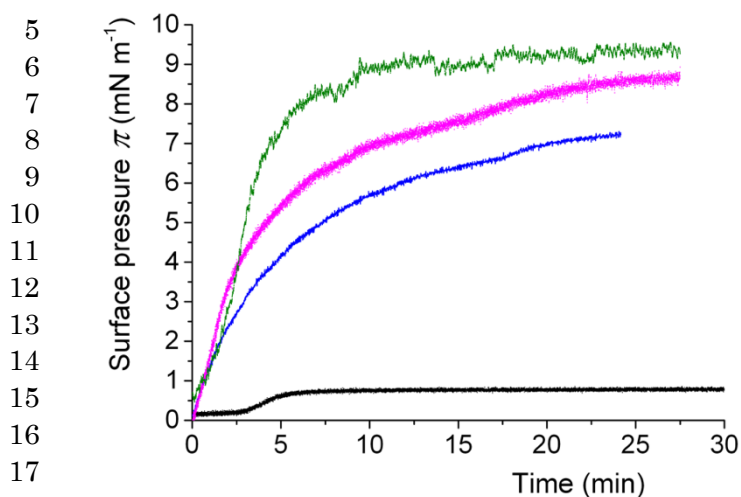
18 **Scheme 3.** Solid-phase synthesis of *F*-lipopeptides **1-3** and hydrocarbon counterpart **4**.

19 Behavior of lipid-peptide conjugates at the air/water interface

20 Spontaneous adsorption of lipid-peptide conjugates at the air/water interface. In

21 order to investigate the capacity for *F*-lipopeptides **1-3** to spontaneously self-assemble
 22 into ordered monolayers at the air/water interface, we injected a solution of each peptide-
 23 lipid conjugates in DMSO into the aqueous sub-phase of an adsorption trough. The
 24 variation of the surface pressure π was measured over time at 25°C (Figure 1). In all cases,
 25 π increased, reflecting a progressive adsorption at the interface, then reached a plateau
 26 and stabilized at the equilibrium surface pressure (π_{eq}). The adsorption kinetics
 27 demonstrate that the *F*-lipopeptides formed stable monolayers at the interface. The π_{eq}
 28 values increased with the degree of fluorination of the *F*-lipopeptides (~ 7.2 mN m⁻¹ for **1**,
 29 8.6 mN m⁻¹ for **2** and 9.4 mN m⁻¹ for **3**; ± 0.5 mN m⁻¹), reflecting their increasingly

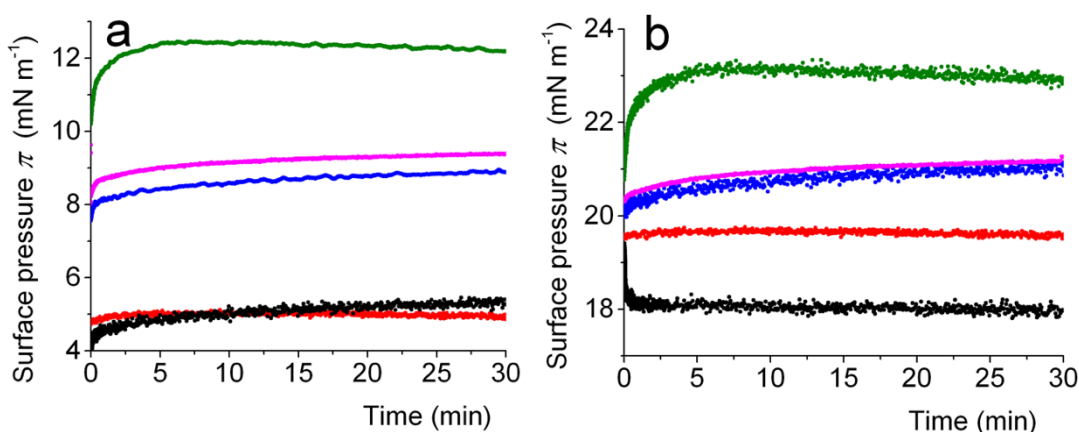
1 hydrophobic character. By contrast, the hydrocarbon analog adsorbed considerably less,
2 reaching a π_{eq} value of only 0.7 mN m^{-1} . The adsorption of the *F*-lipopeptides is also much
3 faster than that of the hydrocarbon compound (characteristic time of adsorption $\tau \sim 0.5$
4 min for **1-3** versus ~ 2.5 min for **4**).



5
6
7
8
9
10
11
12
13
14
15
16
17
18
19 **Figure 1.** Adsorption kinetics of perfluoroalkylated lipopeptides **1-3** and their
20 hydrocarbon analog **4** at the air/water interface (25°C). Variation of surface pressure π as
21 a function of time for **1** (blue), **2** (magenta), **3** (green) and **4** (black).

22 **Adsorption of lipid-peptide conjugates on a phospholipid monolayer spread at the**
23 **air/water interface.** DPPC is widely used in the formulation of liposomes and
24 microbubbles [29, 31]. In order to investigate the ability of *F*-lipopeptides to form mixed
25 monolayers with DPPC at the air/water interface, *F*-lipopeptides were injected in the
26 aqueous sub-phase of a Langmuir monolayer of DPPC. Depending on the volume of
27 DPPC solution deposited, the monolayer is either in the liquid expanded (LE, 5 mN m^{-1})
28 or in the liquid condensed (LC, 19 mN m^{-1}) phase (Figure 2a,b). In the LE phase, π values
29 of *F*-lipopeptides were significantly higher than that of the DPPC monolayer (Figure 2a)
30 and remained stable over time, which means that the lipopeptides are inserted in the DPPC
31 monolayer. On the other hand, injection of the hydrocarbon analog **4** was not followed by

1 an increase of π , which suggests that **4** is not adsorbed in the DPPC monolayer. In the LC
 2 phase, π_{eq} is $\sim 19 \text{ mN m}^{-1}$ for DPPC alone. We observed that π_{eq} increased significantly
 3 after injection of the *F*-lipopeptides, reflecting their insertion in the DPPC monolayer.
 4 The higher the degree of fluorination, the higher the amount inserted, with maximal
 5 efficiency observed for **3**. The behavior of the hydrocarbon lipopeptide **4** was markedly
 6 different, with a decrease of surface pressure over time, and a much lower π_{eq} . This, not
 7 only means that the hydrocarbon analog is not recruited at the interface, but also that there
 8 is a significant loss of molecules, and that contact of the hydrocarbon lipid with the DPPC
 9 monolayer causes a delipidation of the interface.

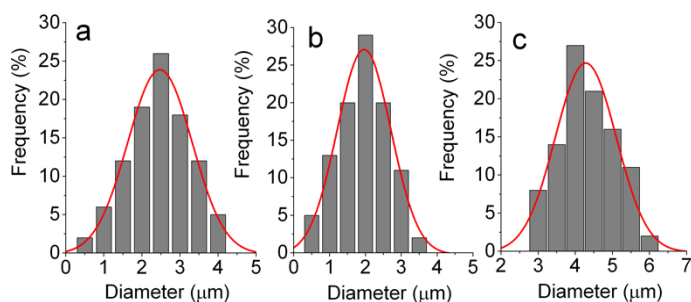


24 **Figure 2.** Adsorption of perfluoroalkylated lipopeptides **1-3** and hydrocarbon analog **4**
 25 on DPPC monolayers spread at the air/water interface a) in the liquid expanded (LE) and
 26 b) in the liquid condensed (LC) phases (25°C). Variation of surface pressure π as a
 27 function of time for a DPPC monolayer (red), and after injection of the lipopeptides in
 28 the aqueous sub-phase of a DPPC monolayer for *F*-lipopeptides: **1** (blue), **2** (magenta), **3**
 29 (green) and hydrocarbon analog **4** (black).

30 Generation of microbubbles from combinations of DPPC and lipid-peptide
 31 conjugates

32 Next, we have investigated whether microbubbles incorporating the lipopeptides in

1 their shell could be produced and what their effect on the size characteristics and stability
2 of the resulting MBs would be. We therefore selected DPPC and DPPE-PEG2000 as the
3 main MB shell components. The PEGylated phospholipid is often used in MB
4 formulations to increase MB half-lives. The microbubbles were prepared by mechanical
5 agitation using a Vialmix shaker and were characterized by optical microscopy
6 immediately after preparation and over time. The results show that incorporation of *F*-
7 lipopeptides **1-3** led to MBs that are somewhat smaller than those made from DPPC alone
8 (e.g. $1.9 \pm 0.6 \mu\text{m}$ with *F*-lipopeptide **3** versus $2.5 \pm 0.8 \mu\text{m}$ without, Figure 3a,b).
9 Microbubbles with similar mean diameters were obtained with the two other *F*-
10 lipopeptides. By contrast, incorporation of the hydrocarbon analog **4** led to a marked
11 increase in mean MB diameter ($4.3 \pm 0.9 \mu\text{m}$, Figure 3c).

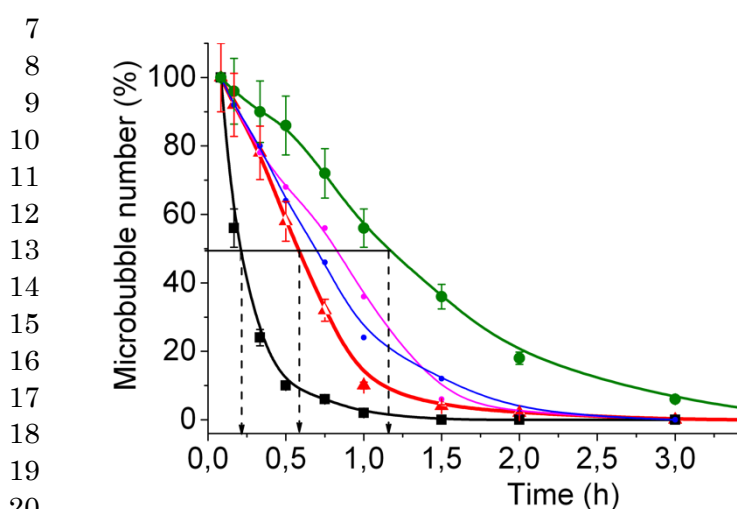


12
13
14
15
16
17
18
19
20
21
22 **Figure 3.** Size distribution of perfluorohexane-stabilized microbubbles with a shell of a)
23 DPPC, b) DPPC/*F*-lipopeptide **3** and c) DPPC/hydrocarbon analog **4**.

24 Finally, we have investigated the stability of the microbubbles over time at room
25 temperature. The MBs containing *F*-lipopeptides were found to be more stable than the
26 reference DPPC/DPPE-PEG2000 MBs (Figure 4). The most stable MBs were those
27 containing *F*-lipopeptide **3** with a half-life of 1.1 ± 0.2 h, as compared to 0.6 ± 0.2 for
28 DPPC MBs. MBs incorporating *F*-lipopeptides 1 and 2 displayed intermediate half-lives.

29 The reduction in size of MBs incorporating *F*-lipopeptides compared to those

1 incorporating the hydrocarbon compound **4** can be explained by the faster diffusion of the
 2 former lipopeptides to the interface and by their larger value of π_{eq} , hence lower surface
 3 tension at the bubble surface. The enhanced MB stability over time and the fact that their
 4 half-life increases with fluorocarbon chain length support the view that stabilizing
 5 interactions develop between *F*-lipopeptide and perfluorohexane in the bubble's
 6 interfacial film.



21 **Figure 4.** Half-lives of microbubbles (25°C) containing *F*-lipopeptides **1-3** and
 22 hydrocarbon analog **4**.

23 Conclusions and Perspectives

24 A series of lipopeptides carrying C_nF_{2n+1} chains ($n = 6, 7, 8$, **1-3**) or $C_{10}H_{21}$ chains (**4**)
 25 grafted through a lysine moiety on a peptide chain composed of a KSS sequence followed
 26 by 5 SG sequences were synthesized by Fmoc solid-phase peptide synthesis. Investigation
 27 of the physicochemical properties of these lipopeptides at the air/water interface
 28 demonstrates that fluorination substantially improves their surface-active properties. In
 29 our experimental conditions, fluorination enables significantly larger and faster
 30 adsorption, both at the surface of water and on DPPC monolayers in both the LE and LC
 31 states. By contrast, adsorption of the hydrocarbon analog is only possible when the

1 phospholipid monolayer in the LE state, whilst its adsorption in the LC state is not only
2 prohibited, but even provokes a delipidation of the interface. Incorporation of the
3 perfluoroalkylated lipopeptides in the phospholipid shells of perfluorohexane-stabilized
4 microbubbles significantly reduces their mean size and increases their stability. By
5 contrast, larger bubbles with shorter half-lives are obtained with the hydrocarbon analog.
6 Our results establish that fluorination of these precursors of targeting ligand-peptide
7 conjugates can considerably facilitate microbubble generation due to faster diffusion to
8 the air/water interface, and augment their stability through interfacial fluorine-fluorine
9 interactions.

10 Experimental

11 **Materials.** We purchased Fmoc-protected amino acids, *N,N*-dimethylformamide (DMF),
12 dichloromethane (DCM), methanol, 1-hydroxybenzotriazole (HOBT), 2-(1*H*-
13 benzotriazole-1-yl)-1,1,3,3-tetramethyluronium hexafluorophosphate (HBTU), *N,N*-
14 diisopropylethylamine (DIPEA), piperidine, acetic anhydride, trifluoroacetic acid (TFA),
15 triisopropylsilane (TIS), Rink Amide AM resin (4-(2',4'-dimethoxyphenyl-Fmoc-
16 aminomethyl)-phenoxyacetamido-aminomethyl resin, 100-200 mesh), and Tube-O-
17 DIALYZER™ mini dialysis system (MWCO 1K) from Merck (Darmstadt, Germany).
18 1,2-dipalmitoylphosphatidylcholine (DPPC) (>99%) and 1,2-dipalmitoyl-*sn*-glycero-3-
19 phosphoethanolamine-*N*-[methoxy(polyethylene glycol)-2000] (DPPE-PEG2000)
20 (>99%) were purchased from Avanti Polar Lipids (Alabaster, AL, USA) and used without
21 further purification. Perfluorohexane came from Fluorochem (>98%). A HEPES (N-2-
22 (hydroxyethyl)piperazine-*N'*-(2-ethanesulfonic acid), powder, 99.5%, Corning, NY)
23 buffer solution (20 mM) in 150 mM NaCl was prepared and adjusted to pH 7.4 using 0.1

1 N NaOH. Chloroform (99.4%) was purchased from VWR (Avantor, Fontenay-sous-Bois).
2 Ultrapure water was obtained from a Milli-Q (Millipore Corp.) system (surface tension:
3 72.1 mN m^{-1} at 20°C , resistivity: $18.2 \text{ M}\Omega \text{ cm}$).

4 **General procedure for the synthesis of perfluoroalkylated lipopeptides.** All *F*-
5 lipopeptides $(\text{SG})_5\text{-KSS-K}(\text{C}_2\text{H}_4\text{-C}_n\text{F}_{2n+1})_2$ with $n = 6$ (**1**), 7 (**2**) and 8 (**3**) and hydrocarbon
6 analog $(\text{SG})_5\text{-KSS-K}(\text{C}_{10}\text{H}_{21})_2$ were synthesized using a Fmoc solid-phase peptide
7 synthesis (SPPS) method. Rink Amide AM resin (0.1 mmol) in a 10 mL column was
8 suspended in 5 mL of DMF and swollen overnight. After washing with DMF ($3 \times 2 \text{ mL}$),
9 the Fmoc groups of Rink amide AM resin were activated with 20% of piperidine in DMF
10 (2 mL) for 20 min. After washing with DMF ($3 \times 2 \text{ mL}$), Fmoc-Ser(tBu)-OH (3 eq.) as
11 the first Fmoc-amino acid and the mixture of HBTU, HOBT, and DIPEA (3 eq./3 eq./6
12 eq.) in DMF were added to the resin and shaken for 30 min. The reaction was monitored
13 using a Kaiser test based on the reaction of ninhydrin. After washing with DMF (3×2
14 mL) and DCM ($3 \times 2 \text{ mL}$), 25% of acetic anhydride in DCM (2 mL) was added for
15 capping the unreacted amino acids and the mixture was shaken for 5 min. In a similar
16 manner, each of the peptide chains was elongated by coupling Fmoc-Ser(tBu)-OH (3 eq.),
17 Fmoc-Gly-OH (3 eq.) and Fmoc-Lys(Boc)-OH (3 eq.) to Rink Amide AM resin. After
18 introducing Fmoc-Lys(Fmoc)-OH as the terminal amino acid, the Fmoc groups of Fmoc-
19 Lys(Fmoc)-OH were activated with $2 \times 20\%$ of piperidine in DMF (2 mL) for 20 min,
20 and the coupling reaction with perfluoroalkylated acids (3 eq.) or alkyl acid (3 eq.) was
21 performed 3 times with HBTU/HOBT/DIPEA (6 eq./6 eq./12 eq.) for 3 h. After capping
22 the reaction with 25% of acetic anhydride in DCM (2 mL), the column was washed with
23 DCM ($3 \times 2 \text{ mL}$), DMF ($3 \times 2 \text{ mL}$) and methanol ($3 \times 2 \text{ mL}$), and was dried overnight. A
24 solution of 2.5 mL of TFA/TIS/ H_2O (94/2.5/2.5, v/v/v) was added to the column for

1 cleaving the compound from the resin, and the reaction was performed for 3 h. The
2 TFA/TIS/H₂O solution including the crude product was collected in a 50 mL erlenmeyer
3 flask. The column was washed 3 times with TFA (1.5 mL), and the washing solutions
4 were combined. After drying the solution with argon gas, the residue was washed with 20
5 mL of diethyl ether. The product was collected by filtration and purified by dialysis using
6 a Tube-O-DIALYZER™ mini dialysis system. The purity of final products was analyzed
7 by a high-performance liquid chromatography (HPLC) system using a reversed-phased
8 column (COSMOSIL 5C18-AR-II 4.6 × 250 mm) with water and acetonitrile (20/80 v/v)
9 at a flow rate of 0.5 mL/min.

10 **(SG)₅-KSS-K(C₂H₄-C₆F₁₃)₂ 1** was synthesized according to the general procedure using
11 4,4,5,5,6,6,7,7,8,8,9,9,9-tridecafluorononanoic acid. Yield: 121 mg (6.3%), MS
12 (FAB/MS) m/z: 1916 (M+H)⁺, HRMS 1916.5509 (Calcd. 1916.5511 for
13 C₆₁H₈₄F₂₆N₁₇O₂₃). Purity (retention time): > 99% (13.8 min).

14 **(SG)₅-KSS-K(C₂H₄-C₇F₁₅)₂ 2** was synthesized according to the general procedure using
15 4,4,5,5,6,6,7,7,8,8,9,9,10,10,10-pentadecafluorodecanoic acid. Yield: 95 mg (4.7%), MS
16 (FAB/MS) m/z: 2016 (M+H)⁺, HRMS 2016.5448 (Calcd. 2016.5447 for
17 C₆₃H₈₄F₃₀N₁₇O₂₃). Purity (retention time): > 99% (14.8 min).

18 **(SG)₅-KSS-K(C₂H₄-C₈F₁₇)₂ 3** was synthesized according to the general procedure using
19 4,4,5,5,6,6,7,7,8,8,9,9,10,10,11,11,11-heptadecafluoroundecanoic acid. Yield: 111 mg
20 (5.2%), MS (FAB/MS) m/z: 2116 (M+H)⁺, HRMS 2116.5381 (Calcd. 2116.5383 for
21 C₆₅H₈₄F₃₄N₁₇O₂₃). Purity (retention time): > 99% (13.8 min).

22 **(SG)₅-KSS-K(C₁₀H₂₁)₂ 4** was synthesized according to the general procedure using
23 undecanoic acid. Yield: 70 mg (4.7%), MS (FAB/MS) m/z: 1504 (M+H)⁺, HRMS
24 1504.8585 (Calcd. 1504.8586 for C₆₅H₁₁₈N₁₇O₂₃). Purity (retention time): > 99% (13.9

1 min).

2 **Adsorption kinetics of lipopeptides at the air/water interface.** The experiments were
3 conducted in a home-made Teflon adsorption trough (11.9 x 5.0 x 0.3 cm³) filled with
4 HEPES buffer (pH 7.4). The surface pressure π was measured using the Wilhelmy plate
5 method. The temperature was maintained at 25 ± 0.5 °C. For the spontaneous formation
6 of monolayers (Gibbs films) at the air/water interface, 50 μ L of solutions of the
7 lipopeptides **1-4** in DMSO (1 mmol L⁻¹) were injected into the aqueous phase. For the
8 experiment concerning the adsorption of lipopeptides on a DPPC Langmuir monolayer, a
9 solution of DPPC in chloroform (1 mmol L⁻¹) was deposited on the surface of the aqueous
10 phase. Depending on the volume deposited (9 μ L or 18 μ L), DPPC monolayers were
11 obtained in the liquid expanded or in the liquid condensed phase. 10 min were allowed to
12 evaporate chloroform. 50 μ L of solutions (1 mmol L⁻¹) of lipopeptides in DMSO were
13 then injected in the aqueous sub-phase and the surface pressure was monitored over time.
14 Three separate experiments were conducted for each lipopeptide. The error made on
15 surface pressure measurements is ± 0.5 mN m⁻¹.

16 **Preparation and characterization of lipopeptide-containing microbubbles.** DPPC (50
17 mmol L⁻¹) and DPPE-PEG2000 (DPPC/DPPE-PEG2000 molar ratio 9:1) were dispersed
18 in a HEPES buffer solution (0.9 mL) by magnetic stirring for 3-6 h at 50°C. 50 μ L of the
19 lipopeptide solution in DMSO were injected into the phospholipid dispersion and
20 subjected to agitation/amalgamation using a Vialmix® device (2 cycles of 45 s, Lantheus
21 Medical Imaging N. Billerica, MA) at room temperature and under *F*-hexane-saturated
22 N₂ at room temperature (for details, see [37]). The resulting foam was immediately diluted
23 with 5 mL of HEPES buffer. Size fractionation of the microbubbles was achieved by
24 flotation for 60 min. Reference microbubbles shelled with DPPC/DPPE-PEG2000 were

1 prepared using the same protocol. Two to three droplets of bubble dispersion were placed
2 into a concave glass slide, covered with a glass slide and observed with a Nikon Eclipse
3 90i microscope (transmission mode, Nikon Instruments Europe, Amsterdam, The
4 Netherlands). Rapid image acquisition was achieved using a Lumenera Infinity 2 charge-
5 coupled device (CCD) camera (Lumenera, Ottawa, Canada). Bubble mean diameter and
6 distribution width after preparation and upon time were determined on 5–10 slides using
7 *Fiji* (an open-source image processing package[41]) and the standard deviations were
8 calculated using Origin9 (OriginLab Corp. Northampton, MA, USA).

9 Supporting Information

10 Mass spectrometry data and RP-HPLC chromatograms of lipopeptides (1-4).

11 Funding

12 The work was supported by JSPS KAKENHI Grant Number JP18KK0439 and
13 JP20K08139. We also acknowledge CONACYT (Mexico) for a Ph.D fellowship
14 (E.E.M.O., grant #459199).

15 References

- 16 1. Ferrara, K. W.; Borden, M. A.; Zhang, H. Lipid-shelled vehicles: Engineering
17 for ultrasound molecular imaging and drug delivery *Acc. Chem. Res.* **2009**, *42*, 881-892.
- 18 2. Sercombe, L.; Veerati, T.; Moheimani, F.; Wu, S. Y.; Sood, A. K.; Hua, S.
19 Advances and challenges of liposome assisted drug delivery *Front. Pharmacol.* **2015**, *6*,
20 286.
- 21 3. Su, S.; Kang, P. M. Recent advances in nanocarrier-assisted therapeutics delivery
22 systems *Pharmaceutics* **2020**, *12*, 837.
- 23 4. Siemer, S.; Wunsch, D.; Khamis, A.; Lu, Q.; Scherberich, A.; Krafft, M. P.;

- 1 Hagemann, J.; Weiss, C.; Ding, G.-B.; Stauber, R. H.; Gribko, A. Nano meets micro-
2 translational nanotechnology in medicine: Nano-based applications for early tumor
3 detection and therapy *Nanomaterials* **2020**, *10*, 383.
- 4 5. Chowdhury, S. M.; Abou-Elkacem, L.; Lee, T.; Dahl, J.; Lutz, A. M. Ultrasound
5 and microbubble mediated therapeutic delivery: Underlying T mechanisms and future
6 outlook *J. Control. Release* **2020**, *326*, 75–90.
- 7 6. Osei, E.; Al-Asady, A. A review of ultrasound-mediated microbubbles
8 technology for cancer therapy: A vehicle for chemotherapeutic drug delivery *J. Radiother.*
9 *Pract.* **2020**, *19*, 291-298.
- 10 7. Noble, G. T.; Stefanick, J. F.; Ashley, J. D.; Kiziltepe, T.; Bilgicer, B. Ligand-
11 targeted liposome design: challenges and fundamental considerations *Trends Biotechnol.*
12 **2014**.
- 13 8. Li, J.; Tan, T.; Zhao, L.; Liu, M.; You, Y.; Zeng, Y.; Chen, D.; Xie, T.; Zhang, L.;
14 Fu, C.; Zeng, Z. Recent advancements in liposome-targeting strategies for the treatment
15 of gliomas: A systematic review *ACS Appl. Bio Mater.* **2020**, *3*, 5500–5528.
- 16 9. Bae, K. H.; Chung, H. J.; Park, T. G. Nanomaterials for cancer therapy and
17 imaging *Mol. Cells* **2011**, *31*, 295-302.
- 18 10. Tang, K.; Zhang, Y.; Zhang, H.; Xu, P.; Liu, J.; Ma, J.; Lv, M.; Li, D.; Katirai, F.;
19 Shen, G.-X.; Zhang, G.; Feng, Z.-H.; Ye, D.; Huang, B. Delivery of chemotherapeutic
20 drugs in tumour cell-derived microparticles *Nat. Commun.* **2012**, *1282*.
- 21 11. Wang, H.; Wu, L.; Sun, X. Intratracheal delivery of nano- and microparticles and
22 hyperpolarized gases. A promising strategy for the imaging and treatment of respiratory
23 disease *Chest* **2020**, *157*, 1579-1590.
- 24 12. Wang, S.; Hossack, J.; Klibanov, A. L. Targeting of microbubbles: contrast

- 1 agents for ultrasound molecular imaging. *J. Drug Target.* **2018**, *26*, 420-434.
- 2 13. Hagimori, M.; Fuchigami, Y.; Kawakami, S. Peptide-based cancer-targeted DDS
3 and molecular imaging *Chem. Pharm. Bull.* **2017**, *65*, 618–624.
- 4 14. Wang, J.; Fang, T.; Li, M.; Zhang, W.; Zhang, Z.-P.; Zhang, X.-E.; Li, F.
5 Intracellular delivery of peptide drugs using viral nanoparticles of bacteriophage P22:
6 Covalent loading and cleavable release *J. Mater. Chem. B* **2018**, *6*, 3716-3726.
- 7 15. Isidro-Llobet, A.; Kenworthy, M. N.; Mukherjee, S.; Kopach, M. E.; Wegner, K.;
8 Gallou, F.; Smith, A. G.; Roschangar, F. Sustainability challenges in peptide synthesis
9 and purification: From R&D to production *J. Org. Chem.* **2019**, *84*, 4615–4628.
- 10 16. Molek, P.; Strukelj, B.; Bratkovic, T. Peptide phage display as a tool for drug
11 discovery: Targeting membrane receptors *Molecules* **2011**, *16*, 857-887.
- 12 17. Wang, Q.; Ma, X.; Jia, J.; Fei, H. A peptide–lipid nanoparticle assembly platform
13 with integrated functions for targeted cell delivery *J. Mater. Chem. B* **2016**, *4*, 1535-1543.
- 14 18. Wang, C.; Su, L.; Wu, C.; Wu, J.; Zhu, C.; Yuan, G. RGD peptide targeted lipid-
15 coated nanoparticles for combinatorial delivery of sorafenib and quercetin against
16 hepatocellular carcinoma *Drug Dev. Ind. Pharm.* **2016**, *42*, 1938–1944.
- 17 19. Silva, S.; Almeida, A. J.; Vale, N. Combination of cell-penetrating peptides with
18 nanoparticles for therapeutic application: A review *Biomolecules* **2019**, *9*, 22.
- 19 20. Reithmeier, H.; Herrmann, J.; Göpferich, A. Lipid microparticles as a parenteral
20 controlled release device for peptides *J. Control. Release* **2001**, *73*, 339–350.
- 21 21. Lehtinen, J.; Magarkar, A.; Stepniewski, M.; Hakola, S.; Bergman, M.; Róg, T.;
22 Yliperttula, M.; Urtili, A.; Bunker, A. Analysis of cause of failure of new targeting peptide
23 in PEGylated liposome: Molecular modeling as rational design tool for nanomedicine
24 *Europ. J. Pharm. Sci.* **2012**, *46*, 121–130.

- 1 22. Koniev, O.; Wagner, A. Developments and recent advancements in the field of
2 endogenous amino acid selective bond forming reactions for bioconjugation *Chem. Soc.*
3 *Rev.* **2015**, *44*, 5495--5551.
- 4 23. Suga, T.; Kato, N.; Hagimori, M.; Fuchigami, Y.; Kuroda, N.; Kodama, Y.;
5 Sasaki, H.; Kawakami, S. Development of high-functionality and -quality lipids with
6 RGD peptide ligands: Application for PEGylated liposomes and analysis of intratumoral
7 distribution in a murine colon cancer model *Mol. Pharmaceutics* **2018**, *15*, 4481–4490.
- 8 24. Allen, T. M.; Hansen, C.; Martin, F.; Redemann, C.; Yau-Young, A. Liposomes
9 containing synthetic lipid derivatives of poly(ethylene glycol) show prolonged circulation
10 half-lives in vivo *Biochim. Biophys. Acta* **1991**, *1066*, 29-36.
- 11 25. Klivanov, A. L.; Maruyama, K.; Beckerleg, A. M.; Torchilin, V. P.; Huang, L.
12 Activity of amphipathic poly(ethylene glycol) 5000 to prolong the circulation time of
13 liposomes depends on the liposome size and is unfavorable for immunoliposome binding
14 to target *Biochim. Biophys. Acta* **1991**, *1062*, 142-148.
- 15 26. Suga, T.; Fuchigami, Y.; Hagimori, M.; Kawakami, S. Ligand peptide-grafted
16 PEGylated liposomes using HER2 targeted peptide-lipid derivatives for targeted delivery
17 in breast cancer cells: The effect of serine-glycine repeated peptides as a spacer *Int. J.*
18 *Pharm.* **2017**, *521*, 361–364.
- 19 27. Suga, T.; Watanabe, M.; Sugimoto, Y.; Masuda, T.; Kuroda, N.; Hagimori, M.;
20 Kawakami, S. Synthesis of a high functionality and quality lipid with gp130 binding
21 hydrophobic peptide for the preparation of human glioma cell-targeted PEGylated
22 liposomes *J. Drug Deliv. Sci. Technol.* **2019**, *49*, 668–673.
- 23 28. Craig, J. A.; Rexeisen, E. L.; Mardilovich, A.; Shroff, K.; Kokkoli, E. Effect of
24 linker and spacer on the design of a fibronectin-mimetic peptide evaluated via cell studies

- 1 and AFM Adhesion forces *Langmuir* **2008**, *24*, 10282-10292.
- 2 29. Schutt, E. S.; Klein, D. H.; Mattrey, R. M.; Riess, J. G. Injectable microbubbles
3 as contrast agents for diagnostic ultrasound imaging: The key role of perfluorochemicals
4 *Angew. Chem. Int. Ed.* **2003**, *42*, 3218-3235.
- 5 30. Hernot, S.; Klivanov, A. L. Microbubbles in ultrasound-triggered drug and gene
6 delivery *Adv. Drug Deliv. Rev.* **2008**, *60*, 1153-1166.
- 7 31. Sirsi, S. R.; Borden, M. A. State-of-the-art materials for ultrasound-triggered
8 drug delivery *Adv. Drug Deliv. Rev.* **2014**, *72*, 2-14.
- 9 32. Chong, W. K.; Papadopoulou, V.; Dayton, P. A. Imaging with ultrasound contrast
10 agents: current status and future *Abdom. Radiol.* **2018**, *43*, 762-772.
- 11 33. Rossi, S.; Waton, G.; Krafft, M. P. Phospholipid-coated gas bubble engineering
12 - Key parameters for size and stability control as determined by an acoustic method
13 *Langmuir* **2010**, *26*, 1649-1655.
- 14 34. Szijjarto, C.; Rossi, S.; Waton, G.; Krafft, M. P. Effects of perfluorocarbon gases
15 on the size and stability characteristics of phospholipid-coated microbubbles - Osmotic
16 effect versus interfacial film stabilization *Langmuir* **2012**, *28*, 1182-1189.
- 17 35. Yang, G.; O'Duill, M.; Gouverneur, V.; Krafft, M. P. Recruitment and
18 immobilization of a fluorinated biomarker across an interfacial phospholipid film using a
19 fluorocarbon gas *Angew. Chem. Int. Ed.* **2015**, *54*, 8402-8406.
- 20 36. Shi, D.; Wallyn, J.; Nguyen, D.-V.; Perton, F.; Felder-Flesch, D.; Bégin-Colin,
21 S.; Maaloum, M.; Krafft, M. P. Microbubbles decorated with dendronized magnetic
22 nanoparticles for biomedical imaging. Effective stabilization via fluororous interactions
23 *Beilstein J. Nanotechnol.* **2019**, *10*, 2103-2115.
- 24 37. Mendoza-Ortega, E. E.; Dubois, M.; Krafft, M. P. Fluorocarbon gas exposure

1 induces disaggregation of nanodiamond clusters and enhanced adsorption, enabling
2 medical microbubble formation *ACS Appl. Nano Mater.* **2020**, *3*, 8897-8905.

3 38. Nakahara, H.; Lee, S.; Krafft, M. P.; Shibata, O. Fluorocarbon-hybrid pulmonary
4 surfactants for replacement therapy - A Langmuir monolayer study *Langmuir* **2010**, *26*,
5 18256-18265.

6 39. Nguyen, P. N.; Trinh Dang, T. T.; Waton, G.; Vandamme, T.; Krafft, M. P. A
7 nonpolar, nonamphiphilic molecule can accelerate adsorption of phospholipids and lower
8 their surface tension at the air/water interface *ChemPhysChem* **2011**, *12*, 2646-2652.

9 40. Sadtler, V. M.; Jeanneaux, F.; Krafft, M. P.; Rabai, J.; Riess, J. G.
10 Perfluoroalkylated amphiphiles with a monomorpholinophosphate or
11 dimorpholinophosphate polar head group *New J. Chem.* **1998**, *22*, 609-613.

12 41. Nguyen, P. N.; Veschgini, M.; Tanaka, M.; Waton, G.; Vandamme, T.; Krafft, M.
13 P. Counteracting the inhibitory effect of proteins towards lung surfactant substitutes: a
14 fluorocarbon gas helps displace albumin at the air/water interface *Chem. Commun.* **2014**,
15 *50*, 11576-11579.
16